

IV. A similar trend has been reported for some styrene derivatives.¹²

The facility in cyclization leading to the cyclic structure decreased in the order (Table IV):

(metal halide in polar solvent) >
 (metal halide in nonpolar solvent) >
 (oxo acid in polar solvent) >>
 (oxo acid in nonpolar solvent)

This is quite the reverse of that for the transfer constant (Table III). The strength of the interaction between the growing end and the counterion should also follow the above order, and thus it can be concluded that intramolecular cyclization predominates over β -proton elimination when the cation–anion interaction is weakened (vide infra).

Effect of the Methyl Group. *o*-MeSt and *p*-MeSt are more reactive than styrene,^{13,14} and they gave higher oligomers except for *o*-MeSt in C_6H_6 . Another effect of the methyl group is the promotion of cyclization that led to more cyclic end groups than in the styrene oligomerizations (Table IV). The electron-donating methyl group not only weakens the interaction between the growing carbocation and the counterion, but also increases the electron density of the penultimate phenyl group in the cation. Thus, the intramolecular cyclization preceded the β -proton elimination that might need the assistance of the counterion. In *m*-MeSt oligomerizations, the cyclization will be further facilitated by the increased electron density of positions ortho to the methyl group.

The transfer constant for the *o*-MeSt/ $AcClO_4$ system in C_6H_6 was abnormally larger than the corresponding values for *p*-MeSt and *m*-MeSt (Table IV). This difference may be caused by the steric hindrance of the ortho methyl group that disturbs the approach of monomers toward the

cationic site. On the other hand, the peculiarity of *o*-MeSt was not observed in a polar solvent (see Figures 1 and 2 and Table III) or in the reactions by the metal halide catalysts (Figure 3 and Table III). Consequently, it was concluded that the marked steric hindrance of the ortho methyl group operates only when there is a strong interaction between the growing carbocation and the counterion.

In sum, the MWD and structure of the methylstyrene oligomers have revealed clear differences in catalytic behavior between the oxo acids and the metal halides, which can be interpreted consistently in terms of the interaction between the growing carbocation and the counterion.

References and Notes

- (1) T. Higashimura, M. Hiza, and H. Hasegawa, *Macromolecules*, **12**, 217 (1979).
- (2) T. Higashimura and H. Nishii, *J. Polym. Sci., Polym. Chem. Ed.*, **15**, 329 (1977).
- (3) T. Higashimura, *Polym. Prepr., Am. Chem. Soc., Div. Polym. Chem.*, **20** (1), 161 (1979).
- (4) A. R. Taylor, G. W. Keen, and E. J. Eisenbraun, *J. Org. Chem.*, **42**, 3477 (1977).
- (5) J. M. Barton and D. C. Pepper, *J. Chem. Soc.*, 1573 (1964).
- (6) G. Evans et al., *J. Chem. Soc.*, 2982, 4123 (1959); 3532 (1961).
- (7) H. Nishii and T. Higashimura, *J. Polym. Sci., Polym. Chem. Ed.*, **15**, 1179 (1977).
- (8) R. F. Nystrom and W. G. Brown, *J. Am. Chem. Soc.*, **69**, 1197 (1947).
- (9) C. S. Marvel and G. L. Schertz, *J. Am. Chem. Soc.*, **65**, 2054 (1943).
- (10) T. Masuda and T. Higashimura, *J. Macromol. Sci., Chem.*, **5**, 547 (1971).
- (11) S. W. Ela and D. J. Cram, *J. Am. Chem. Soc.*, **88**, 5777 (1966).
- (12) R. Wolovsky and N. Maoz, *J. Org. Chem.*, **38**, 4040 (1973).
- (13) C. G. Overberger, L. H. Arond, D. Tanner, J. J. Taylor, and T. Alfrey, Jr., *J. Am. Chem. Soc.*, **74**, 4848 (1952).
- (14) C. G. Overberger, T. M. Chapman, and T. Wojnarowski, *J. Polym. Sci., Part A*, **3**, 2865 (1965).

Determination of the Rate Constants of the Elementary Steps in the Cationic Polymerization of Styrene by Trifluoromethanesulfonic Acid¹

Toyoki Kunitake* and Kunihide Takarabe

Department of Organic Synthesis, Faculty of Engineering, Kyushu University, Fukuoka 812, Japan. Received August 6, 1979

ABSTRACT: The cationic polymerization of styrene initiated by CF_3SO_3H was investigated in 1,2-dichloroethane at -1 to $30^\circ C$ by the stopped flow/rapid scan spectroscopy which was combined with the rapid quenching technique. The rate constants of the elementary steps, initiation (k_i), propagation (k_p), spontaneous transfer and termination (k_t), and transfer to monomer (k_{tm}), were determined at four temperatures on the basis of the time courses of the cation formation, monomer consumption, and molecular weight of the quenched polymer. The k_p value varied from 5×10^4 to $2 \times 10^5 M^{-1} s^{-1}$ in the temperature range studied, and k_t was 100 – $300 s^{-1}$. The lifetime of the propagating species ranged from 5 to 100 ms. $(n-Bu)_4N^+CF_3SO_3^-$ was added as a common ion salt, but its influence on the rate constants was small. The activation energy as determined from the Arrhenius plots was 7 and 15 kcal/mol for the k_p and k_{tm} processes, respectively. The transfer constants k_{tm}/k_p and k_t/k_p were close to 0.01 at the 0 – $30^\circ C$ range, in agreement with those reported for the H_2SO_4 initiator.

Fundamental kinetics of the cationic polymerization of vinyl monomers remained unsolved for some time because of the inability to detect the short-lived propagating species. Several years ago, however, De Sorgo et al.² observed a transient absorption at 340 nm upon mixing of styrene and perchloric acid at $-80^\circ C$, which they assigned

to the polystyryl cation. Subsequently, kinetic analyses were performed for the complex polymerization behavior of this system.^{3,4} We have similarly observed the absorption of the polystyryl cation, using trifluoromethanesulfonic acid as initiator,⁵ and carried out a preliminary kinetic study based on the direct determination of the

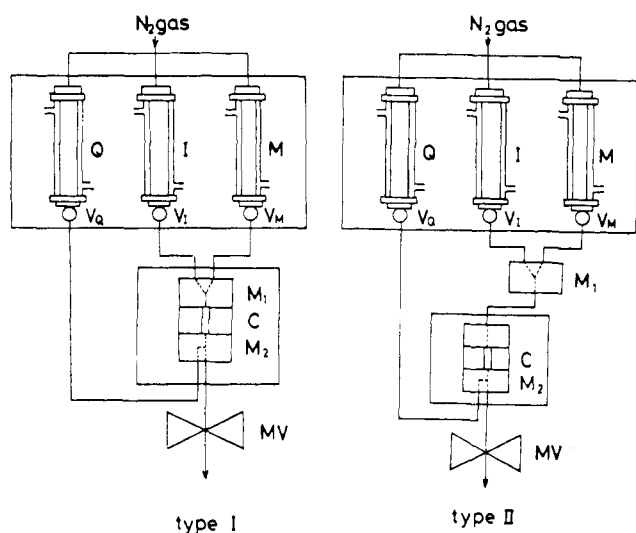


Figure 1. Setup of the stopped-flow and flow apparatus. Type I setting was used for the stopped-flow study and for the quenching experiment with a quenching time of less than 25 ms. Type II setting was used for the quenching experiment with a quenching time of more than 50 ms. Letter identifications: M, I, Q, reservoirs for monomer (M), initiator (I), and quenching solution (Q); V, needle valve; M_1 , jet mixer; M_2 , mixer; and MV, magnetic valve.

propagating species.⁶ The $\text{CF}_3\text{SO}_3\text{H}$ -styrene system appears to be advantageous over the HClO_4 -styrene system for detailed kinetic analyses, since there is no ambiguity concerning the carbocationic nature of the propagating species.

In this paper, we describe the kinetic analysis of the elementary steps of this system: initiation, propagation, chain transfer, and termination.

Recently, Sawamoto and Higashimura also started stopped-flow studies on the cationic polymerization process of *p*-methoxystyrene.^{7,8}

Experimental Section

Materials. Commercial styrene was washed and distilled from CaH_2 under nitrogen. Trifluoromethanesulfonic acid (Wako Pure Chemical Industry) was used without further purification. Dichloroethane solvent was washed, dried over CaCl_2 , and fractionally distilled from P_2O_5 . After repeated distillation from CaH_2 , the distillate was stored over Molecular Sieve 4A. Tetra-*n*-butylammonium trifluoromethanesulfonate was prepared according to the procedure of Sawamoto et al.⁹ and recrystallized two times from a mixed solvent of ethyl acetate and *n*-hexane: yield 70%, mp 114–116 °C (lit.⁹ mp 114–115 °C).

Kinetic Procedures. The initiator and monomer solutions were prepared under dry nitrogen by the syringe technique or in a drybox. The reaction was followed by a stopped-flow/rapid-scan spectrophotometer (Union Giken Co., Model RA 1300). The spectral observation and quenching of the polymerization mixture were conducted separately in the previous experiments.⁶ In the present study, however, modifications were made by the use of a special attachment (Union Giken Co., RA 416) in such a way as to be able to carry out the stopped-flow and flow (quenching) studies in the same apparatus; see Figure 1.

Three jacketed reservoirs (capacity, 15 mL) were fixed in a box which was thermally insulated by Urethane foam. Needle valves were attached at the outlet of these reservoirs in order to control the flow rate. The reservoirs were washed thoroughly with purified dichloroethane and flushed with dry nitrogen. In the stopped-flow mode, dry dichloroethane was placed in reservoir Q, needle valve V_Q was opened, and the photocell unit was filled with solvent by opening the magnetic valve MV. The photocell unit was composed of cell compartment C and two mixers M_1 and M_2 placed before and after the photocell. Monomer and initiator solutions were placed in reservoirs M and I, respectively. The needle valves

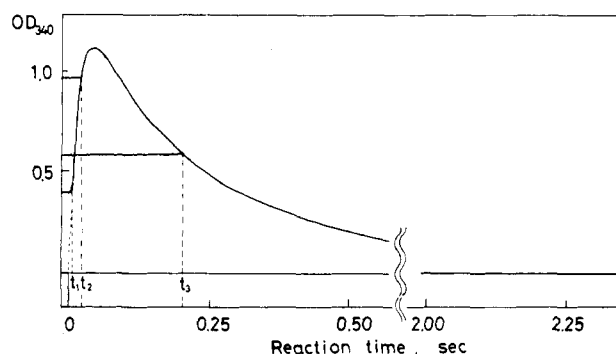


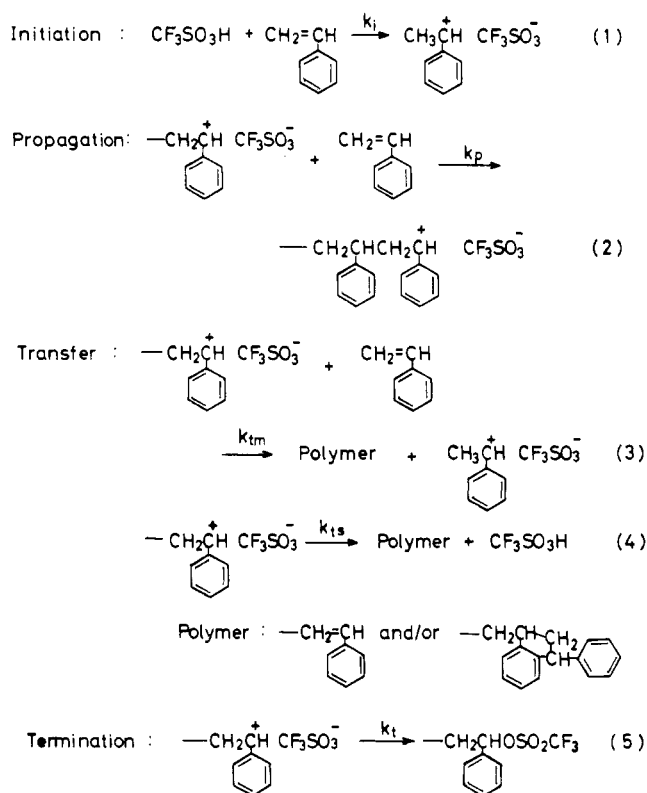
Figure 2. Stopped-flow spectra. Polymerization conditions: -1 °C, dichloroethane solvent, $[\text{CF}_3\text{SO}_3\text{H}] = 2.5$ mM, $[\text{styrene}] = 0.305$ M. Three spectra are superimposed. The respective spectra start at t_1 (dead time = 2–3 msec, nitrogen pressure 6 kg/cm² with the type I setting), at t_2 (dead time = 24 ms, nitrogen pressure 1.5 kg/cm² with the type I setting), and at t_3 (nitrogen pressure 1.5 kg/cm²; the distance between M_1 and C is 4.5 cm in the type II setting).

attached to M and I were kept closed at this time. The reservoirs were maintained at a given polymerization temperature, usually for 10 min, by circulating water from a constant temperature bath. V_M and V_I were opened under nitrogen pressure (V_Q was kept closed). Then, by magnetically opening MV, the two solutions were mixed by jet mixer M_1 which was directly connected to photocell C, and spectra were recorded in the magnetic memory. An oscilloscope monitor was used. The jet mixer M_1 and the photocell C are separated by 0.7 mm in the type I setting. Therefore, the spectral change due to reaction begins to be seen some time later than the actual mixing. This time lapse between mixing and the start of the spectral change at the cell is called "dead time". The dead time depended on the nitrogen pressure applied and, in the type II setting, the distance of Diflon tubing which connects the first jet mixer and the photocell. When the maximal nitrogen pressure (6 kg/cm²) was applied in the type I setting, most of the spectral change could be observed because of the shortest dead time (2–3 ms). Typical spectral change at 340 nm is shown in Figure 2. The absorbance change was extrapolated to the zero absorbance which was equal to the absorbance at infinite time, in order to determine the start time. When the nitrogen pressure was lowered or when the type II setting was used, the dead time was longer, and only the latter portions of the spectral change were observed under the same reaction conditions: cf. runs 2 and 3 in Figure 2. The dead times were determined by superimposing these spectra on the first spectrum (with the shortest dead time) and finding the spectral position of $t = 0$ for each spectrum.

MV was kept open for the period sufficient for a newly-mixed solution to completely replace the solution of the previous run in the photocell. This was controlled by the duration time dial (<1 s in the stopped-flow mode), and complete replacement was confirmed by the observation of normal rapid-scan spectra.

In the flow (quenching) experiment, type I or type II settings were used depending on whether the quenching time was shorter than 25 ms or longer than 50 ms. Ten milliliters each of the solutions of monomer, initiator, and quencher were placed in the respective reservoirs under nitrogen. After the temperature equilibrium was attained (usually less than 10 min), needle valves V_M , V_I , and V_Q were opened. Immediately, magnetic valve MV was opened, and all the solutions were allowed to flow. The flow rate from each reservoir was controlled to be the same by needle valves. Since the quenching solution is mixed immediately after the reaction mixture has passed the photocell (the path length between the photocell C and the quenching mixer M_2 was ca. 10 mm), the quenching time was approximately equal (within a few milliseconds) to the dead time determined in the stopped-flow mode. The quenched mixture was subjected to the same workup as mentioned before, and the residual monomer and the molecular weight of the polymer were determined by UV spectroscopy and gel permeation chromatography, respectively.⁶ The change in the monomer concentration during polymerization was determined from the residual monomer. The spectroscopic method could not

Scheme I



be used because relatively high monomer concentrations were used.

Attempted Detection of Sulfonate End Group. An attempt was made to determine the trifluoromethanesulfonate ester end group which would be formed by coupling with the counteranion by fluorine analysis (Alizarin Complexan method).¹⁰ The fluoride group could not be detected in the polymers quenched by CH_3ONa in CH_3OH and by CH_3OH (experimental error, 0.01 wt %).

Results and Discussion

Polymerization Process. It was shown in our previous paper⁶ that the cationic polymerization of styrene by $\text{CF}_3\text{SO}_3\text{H}$ initiator proceeded cleanly at 30 °C for the initial 200–300 ms period without any UV spectroscopic indication of side reactions. The initiation rate was proportional to the initiator concentration and roughly first order with respect to the monomer concentration, although the amount of the polystyryl cation formed was only 1–4% of the total acid concentration. Therefore, the initiation reaction is most probably the simple protonation of styrene. The propagation step is the addition of polystyryl carbocation (or its trifluoromethanesulfonate salt) to styrene.

The two kinds of chain end structure were identified in the HClO_4 -initiated polymerization of styrene in dichloroethane:¹¹ one is the unsaturated terminal and the other is the phenylindane terminal formed by the attack of the propagating cation on the penultimate phenyl ring. These chain ends may be formed either by transfer to monomer (k_{tm}) or by spontaneous transfer (k_{ts}).

The transfer to solvent has been noted in the case of aromatic solvents^{12–14} and of various oxygen-containing compounds¹⁵ but can be neglected for dichloroethane solvent. The transfer reaction to polymer is conceivable;^{16–18} however, this process will be unimportant in the fast polymerization by $\text{CF}_3\text{SO}_3\text{H}$ initiator in the absence of contrary evidence. The termination reaction may occur by the formation of the sulfonate ester with the counteranion.

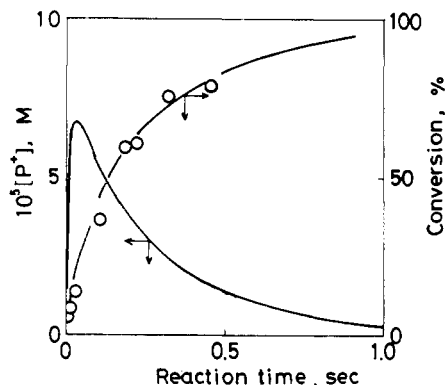


Figure 3. Time course of the formation of styryl cation and conversion. Polymerization conditions: 10 °C; dichloroethane solvent; $[\text{CF}_3\text{SO}_3\text{H}] = 2.4 \text{ mM}$; $[\text{styrene}] = 0.391 \text{ M}$.

Therefore, the reactions in Scheme I will be included as the predominant steps in the polymerization process initiated by $\text{CF}_3\text{SO}_3\text{H}$.

Determination of Rate Constants. The rate constant of initiation, k_i , can be determined from the initial rate of formation of the styryl cation, P^+

$$R_i = (d[\text{P}^+]/dt)_{t=0} = k_i[\text{M}]_0[\text{I}]_0 \quad (6)$$

where M and I denote monomer and initiator, respectively.

On the other hand, the concentration of the polystyryl cation is determined in the whole polymerization range by the rate difference of the formation and disappearance of the propagating species.

$$d[\text{P}^+]/dt = R_i - R_t = k_i[\text{M}][\text{I}] - k_t[\text{P}^+] \quad (7)$$

where

$$k_t = k_{ts} + k_{tm} \quad (8)$$

The polystyryl cation disappears either by the spontaneous splitting of $\text{CF}_3\text{SO}_3\text{H}$ (k_{ts} process) or by the ester formation with the counteranion (k_t process), and these two processes cannot be differentiated kinetically, because the initiator consumption is quite small relative to its total concentration (1–4%).

Thus, assuming that $[\text{I}] = \text{constant} (= [\text{I}]_0)$, integration of eq 7 gives

$$[\text{P}^+] = k_i[\text{I}]_0 \int_0^t [\text{M}] dt - k_t \int_0^t [\text{P}^+] dt \quad (9)$$

$$\therefore \frac{[\text{P}^+]}{\int_0^t [\text{P}^+] dt} = k_i[\text{I}]_0 \frac{\int_0^t [\text{M}] dt}{\int_0^t [\text{P}^+] dt} - k_t \quad (10)$$

The plots of eq 10 give $k_i[\text{I}]_0$ and $-k_t$ from the slope and intercept, respectively.

The rate constant of propagation k_p can be readily determined using $[\text{P}^+]$ and the monomer consumption (conversion) from either of the following equations.⁶

$$\ln ([\text{M}]_{t_1}/[\text{M}]_{t_2}) = k_p \int_{t_1}^{t_2} [\text{P}^+] dt \quad (11)$$

$$\ln ([\text{M}]_{t_1}/[\text{M}]_{t_2}) = k_p [\text{P}^+] \Delta t \quad (12)$$

where $\Delta t = t_2 - t_1$. Equation 12 was applied to the polymerization in the steady state period ($t_1 \sim t_2$) where $[\text{P}^+]$ remained constant. k_p was also estimated graphically from the nonsteady-state portion by using eq 11.

Figure 3 is an example of the variation of $[\text{P}^+]$ and conversion with reaction time at 10 °C. Equation 11 was

Table I
Rate Constants of Styrene Polymerization at 10 °C

[CF ₃ SO ₃ H], mM	[styrene], M	k_i^a , M ⁻¹ s ⁻¹	k_i^b , M ⁻¹ s ⁻¹	$([P^+]_{\max}/[CF_3SO_3H]) \times 100$	$10^{-5}k_p^c$, M ⁻¹ s ⁻¹	$k_{t'}^b$, s ⁻¹	$k_{t'}^d$, s ⁻¹	k_{tm}^d , M ⁻¹ s ⁻¹
2.4	0.391	8	16	2.8	0.89	180	800	1000
6.9	0.305	14	11	3.7	0.81	90	500	900
3.8	0.397	13	13	4.6	0.70	160	800	100

^a Determined by eq 6. ^b Determined by eq 10. ^c Determined by eq 11. ^d Determined by eq 14. The values of $k_{t'}$ and k_{tm} may be the upper and lower limits, respectively; see ref 19.

Table II
Rate Constants of Styrene Polymerization

polymn temp, °C	no. of runs	k_i^a , M ⁻¹ s ⁻¹	k_i^b , M ⁻¹ s ⁻¹	$10^{-5}k_p^c$, M ⁻¹ s ⁻¹	$k_{t'}^b$, s ⁻¹	$k_{t'}^d$, s ⁻¹	k_{tm}^d , M ⁻¹ s ⁻¹
-1	3	5-6	8-10	0.45-0.57	54-180	200-400	200-600
10	3	8-14	13-16	0.70-0.89	90-180	500-800	100-1000
20	4	10-23	13-34	1.1-1.4	170-280	1000-2000	1000-4000
30	5	20-40	11-28	1.6-2.5	220-300	2000-3000	4000-10000

^a Determined by eq 6. ^b Determined by eq 10. ^c Determined by eq 11. ^d Determined by eq 14. The values of $k_{t'}$ and k_{tm} may be the upper and lower limits, respectively; see ref 19.

Table III
Degree of Polymerization of Polystyrene Recovered at Progressive Conversions

polymn temp, °C	no. of runs	[CF ₃ SO ₃ H], ^a mM	[styrene], ^a M	range of conversion, ^b %	\bar{P}_n change ^b
-1	4	2.5-9.8	0.31-0.40	5 → 97	37 → 21
10	3	2.4-6.9	0.31-0.40	8 → 78	31 → 16
20	5	3.8-7.1	0.27-0.40	18 → 93	22 → 10
30	4	2.9-5.8	0.40	18 → 75	16 → 12

^a The range of the initial concentrations used is indicated. The relation between the conversion and the molecular weight was determined for each run under fixed, initial concentrations of initiator and monomer. ^b The arrows denote the range of the conversion observed for quenched polymerization mixtures and the corresponding decrease in \bar{P}_n of the recovered polymer.

applied to these data in order to estimate k_p ; see Figure 4. On the other hand, the data of Figure 3 were analyzed according to eq 10 to obtain k_i and $k_{t'}$ values; see Figure 5. Sufficiently linear relations resulted in both cases.

These rate constants are summarized in Table I, together with similar data obtained at different concentrations of initiator and monomer. The k_i values obtained from eq 6 (rate of the cation formation) and from eq 10 show fair agreements. The initiator efficiency $[P^+]_{\max}/[CF_3SO_3H]$ is less than 10% in all cases. k_p is in the range of $(7-9) \times 10^4$ M⁻¹ s⁻¹, and $k_{t'}$ is 100-200 s⁻¹.

Similar experiments were carried out at other temperatures, and the ranges of the rate constants are summarized in Table II. Again, the agreement is fair between the two kinds of k_i values. As expected, all of the rate constants (k_i , k_p , and $k_{t'}$) increase with increasing temperature.

Separation of Rate Constants of Transfer and Termination. In the above-mentioned procedure, the rate constant of transfer to monomer k_{tm} cannot be determined, since this step does not depend on the concentration of the styryl cation. The k_{tm} value is determined by the conventional Mayo plot (eq 13) or its integrated form

$$\frac{1}{\bar{P}_n} = \frac{k_{tm}}{k_p} + \frac{k_{t'}}{k_p} \frac{1}{[M]} \quad (13)$$

according to Schulz and Harborth¹⁸ (eq 14) where $(\bar{P}_n)_t$ is

$$\frac{1}{(\bar{P}_n)_t} = \frac{k_{tm}}{k_p} + \frac{k_{t'}}{k_p} \frac{\ln([M]_0/[M]_t)}{[M]_0 - [M]_t} \quad (14)$$

the degree of polymerization at time t . $(\bar{P}_n)_t$ was determined at various conversions (usually 8-10 data points)

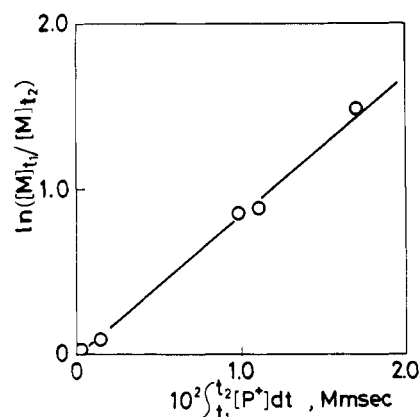


Figure 4. Plots of the data of Figure 3 according to eq 11; $t_1 = 8$ ms.

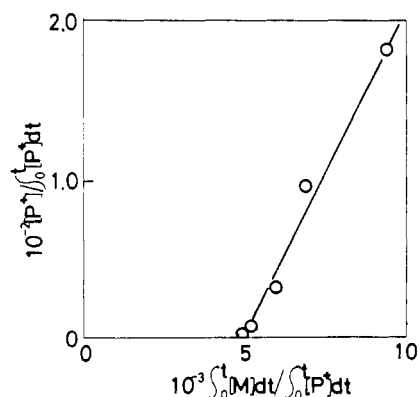


Figure 5. Plots of the data of Figure 3 according to eq 10.

Table IV
Lifetime of Polystyryl Cation in Dichloroethane

polym temp, °C	[CF ₃ SO ₃ H], mM	[styrene], ^a M	10 ⁴ [P ⁺] _{max} , M	10 ³ R _i , ^b M s ⁻¹	10 ³ τ, s
-1	2.9	0.397 (0.28)	1.1	4.5	24
-1	9.8	0.397 (0.17)	9.6	10	96
10	2.4	0.391 (0.34)	0.67	5.7	12
10	6.9	0.305 (0.15)	2.6	15	17
20	4.7	0.397 (0.30)	1.5	33	4.5
20	7.1	0.266 (0.24)	2.5	22	11
30	2.8	0.397 (0.37)	0.39	9.3	4.2
30	5.3	0.315 (0.24)	1.8	36	5.0

^a The initial concentration and the concentration at [P⁺]_{max} (in parentheses) are given. ^b The initiation rate during [P⁺]_{max}.

from gel permeation chromatograms of the quenched polymer by the procedure which was mentioned previously.⁶ The molecular weight decreases gradually with increasing conversions at a given temperature and increases with lowering temperature. Table III summarizes the decrease of \bar{P}_n with conversion under various conditions. \bar{P}_n is 10 to 40 under these conditions. Typical plots of Schulz and Harborth (eq 14) are shown in Figure 6 for a set of data obtained at 10 °C. A sufficiently linear relation (correlation coefficient = 0.999) was found, and k_t/k_p and k_{tm}/k_p were determined from the slope and intercept, respectively. Since k_p is known, k_t and k_{tm} can be calculated. These data are included in Table I. The k_t value determined by Schulz–Harborth plots is generally ca. five times larger than that determined by eq 10. This discrepancy is caused at least partly by the systematic error in the k_t determination by the Schulz–Harborth plots.¹⁹ If this error is taken into consideration, k_t determined by eq 14 becomes smaller by a factor of ca. 2 (i.e., closer to that determined by eq 10), and k_{tm} will become correspondingly larger. Thus k_t determined from eq 10 is considered more reliable, and k_{tm} should be considered to be of an order-of-magnitude accuracy. Similar reproducibilities were noted for k_{tm} and k_t values obtained from eq 14 at other temperatures and are given in Table II.

Separation of k_t into the k_t and k_{ts} terms may be made by determining the sulfonate ester group in the polymer end. The fluorine content was negligible in the quenched polymer. Since the triflate ester may be cleaved readily by the CH₃O⁻ nucleophile, some of the quenching experiment was conducted with methanol, but the fluorine content was again negligible. Therefore, the amount of trifluoromethanesulfonate terminal was estimated to be less than 1% of the total chain end. However, the possibility that the ester linkage is cleaved during the quenching process cannot be discarded completely. In fact, 1-phenylethyl trifluoromethanesulfonate could not be isolated,²⁰ though the 2-phenylethyl isomer has been prepared successfully.²¹ Thus, the separation of the k_{ts} and k_t terms was inconclusive.

Lifetime of the Propagating Species. As can be seen typically in Figure 2, the formation of polystyryl cation shows a maximum after several tens of milliseconds. [P⁺] is fairly constant during this period, and the lifetime of the polystyryl cation τ can be estimated in the steady state by

$$\tau = [P^+]_{\max}/R_i \quad (15)$$

where R_i is the rate of the cation formation during the steady state.

The k_i value was determined from the initial rate of the cation formation under the respective conditions (see Table II). Since the initiator concentration is almost constant during polymerization, R_i at the steady state can be cal-

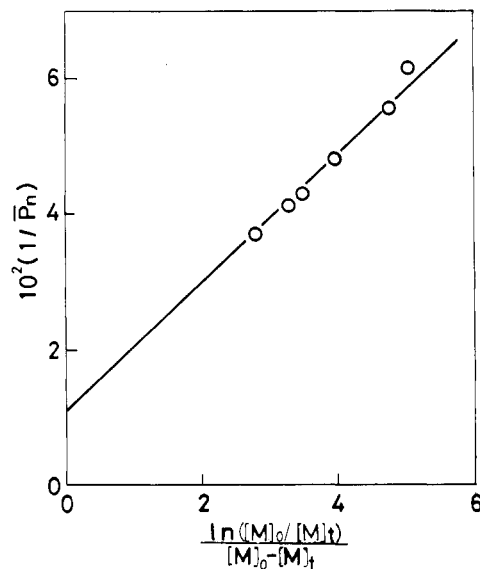


Figure 6. Schulz–Harborth plots (eq 14). The data taken partly from Figure 3.

culated by knowing the monomer concentration during this period; cf. eq 6. Table IV gives selected examples of R_i data and the τ value estimated by eq 15. The lifetime of polystyryl cation is in the range of 5–100 ms in dichloroethane at 0–30 °C and increases with increasing initiator concentrations and with lowering polymerization temperature. The observed effect of the initiator concentration on τ suggests that CF₃SO₃H not only initiates polymerization but also stabilizes the propagating species. This dual role of CF₃SO₃H is consistent with the fact that only a few percent of the CF₃SO₃H molecules is used for initiation in the presence of excess monomer.

Recently Higashimura and Sawamoto²² estimated the τ value for *p*-methoxystyrene to range from 0.2 to several seconds (30 °C, dichloroethane) by the same technique. These lifetimes are much longer than those observed for styrene in the present study, due to the presence of the *p*-methoxy substituent which stabilizes the propagating carbocation.

Common Ion Salt Effect. Table V contains the rate constants determined in the same way as those determined in the presence of a common ion salt: (*n*-Bu)₄N⁺CF₃SO₃⁻. Definite effects cannot be found when the figures of Tables II and V are compared, because the precision of the rate constants is not high. The dissociation constant of the ammonium salt is estimated to be (5–7) × 10⁻⁵ M in the temperature range of 0–30 °C in dichloroethane, and that of the propagating ion pair seems to be smaller.²³ Therefore, addition of 10⁻³–10⁻⁵ M of the common ion salt would be sufficient to shift the dissociation equilibrium of the propagating species toward the ion pair formation.

Table V
 Rate Constants Determined in the Presence of a Common Ion Salt^a

polym temp, °C	no. of runs	k_i^b , M ⁻¹ s ⁻¹	k_p^c , M ⁻¹ s ⁻¹	$10^{-5}k_p^d$, M ⁻¹ s ⁻¹	k_t^c , s ⁻¹	k_t^e , s ⁻¹	k_{tm}^e , M ⁻¹ s ⁻¹
-1	5	5-12	3-10	0.47-0.57	67-90	200-500	100-1000
10	5	5-16	5-17	0.67-0.78	90-240	600-1200	700-1600
20	4	7-26	7-13	1.0-1.4	140-390	1500-1700	1000-1400
30	4	13-28	11-32	1.1-1.4	220-470	2000-3000	5000-6000

^a Common ion salt: (n-Bu)₄N⁺CF₃SO₃⁻, 1.2×10^{-3} - 2×10^{-5} M. ^b Determined by eq 6. ^c Determined by eq 10. ^d Determined by eq 11. ^e Determined by eq 14 (Schulz-Harborh plots).

 Table VI
 Activation Parameters of the Elementary Processes

elementary process	frequency factor, log A	activation energy, kcal/mol
initiation (k_i)	7 ^a (6 ^b)	8 ^a (6 ^b)
propagation (k_p)	10	7
spontaneous transfer and termination (k_t)	6 ^c (12 ^d)	5 ^c (12 ^d)
transfer to monomer (k_{tm})	14	15

^a Based on the k_i value derived from eq 6. ^b Based on the k_i value derived from eq 10. ^c Based on the k_t value derived from eq 10. ^d Based on the k_t value derived from eq 14. These values are less reliable; see text.

The common ion salt effect was clearly observed for the k_p term, as described in detail in the accompanying paper.²³ The other rate constants are supposedly less sensitive to the dissociation equilibrium of the propagating polystyryl cation or, more probably, their limited precisions preclude the detection of the effect of the common ion salt.

Activation Parameters. The activation parameters were determined from the Arrhenius plots of the rate data given in Table II. The average points of the ranges of the rate constant were plotted. The resulting parameters are given in Table VI.

The activation parameters for the k_t process obtained from the two methods do not agree. Since the k_t values derived from eq 10 are more reliable, the small activation parameters ($A = 10^6$ and $E_a = 5$ kcal/mol) are more likely.

The activation energies lie in the same range for initiation, propagation, and spontaneous transfer (and termination). The transfer to monomer possesses a much higher activation energy. Hayes and Pepper²⁴ reported the following activation energies in the H₂SO₄-initiated polymerization of styrene in dichloroethane: propagation, 8.5 kcal/mol; spontaneous transfer and termination, ca. 13 kcal/mol; transfer to monomer, 16 kcal/mol. Their values for propagation and transfer to monomer agree with the corresponding activation energies in our system.

Transfer Constant. The absolute value of the rate constant in the cationic vinyl polymerization has not been determined except for k_p . The k_p data will be discussed in the accompanying paper²³ in comparison with the data given by other workers. Therefore, transfer constants k_{tm}/k_p and k_t/k_p estimated in this study will be compared

here with those in the literature. As shown in Table VII, the k_{tm}/k_p value is approximately 1×10^{-2} in the present system and is comparable to those reported by Hayes and Pepper (H₂SO₄, dichloroethane)²⁴ and by Okamura et al. (TiCl₄, benzene).²⁵ The k_t/k_p value appears somewhat larger in the case of the CF₃SO₃H initiator than in the case of the H₂SO₄ initiator. Anyway, the transfer constants seem to be fairly insensitive to the change of the polymerization condition.

Mechanistic Comparison. The above results indicate that the kinetic data can be accommodated by the most straightforward mechanistic expressions of eq 1-5. The kinetics of the cationic polymerization of styrene by protic acids were studied in the past by several groups of workers, and they usually assumed rather complex initiation mechanisms. Chmelir et al.^{26,27} followed the kinetics of styrene polymerization (CF₃SO₃H initiator, CH₂Cl₂ solvent) by calorimetry. According to their suggestion, an inactive complex of monomer and initiator was formed rapidly; hence the polymerization rate was proportional to the 2.6-3.0th order of the initiator concentration.

These kinetics were derived on the basis of monomer consumption (calorimetry) during the period of 1 to 100 s with the CF₃SO₃H concentration of 10^{-4} M. In contrast, the polymerization was faster in the present study (<1 s) because of higher CF₃SO₃H concentrations (10^{-2} - 10^{-3} M), and the initiation (formation of styryl cation) and the propagation were clean second-order processes.

Supposedly, side reactions occur during the slow polymerization process of Chmelir. We have observed the formation of a new species absorbing at 417 nm after 1 s.⁵ Similarly, the conductivity data of Chmelir²⁶ suggested the formation of the 1-alkyl-3-phenylindanyl cation during the polymerization period, which would certainly make the kinetic treatment less straightforward.

Pepper's group^{3,4} carried out detailed kinetic studies of the styrene polymerization by HClO₄. Their results indicate that the polymerization process was composed of the fast ionic and slow nonionic pathways. This mechanistic duality was not observed in our system, since the whole polymerization range (conversion, ~100%) could be discussed in terms of the simple styryl cation (see Figure 2).

We thus conclude that the fast polymerization of styrene by CF₃SO₃H is advantageous over the other systems in performing the kinetic analysis. This kinetic simplicity

 Table VII
 Transfer Constants

rel rate constant	initiator	solvent	polymerization temp, °C				remarks
			-1	10	20	30	
$(k_{tm}/k_p)10^2$	CF ₃ SO ₃ H	dichloroethane	0.4-0.6	1.0-2.0	0.6-3.5	1.2-4.1	this work
	H ₂ SO ₄ ^a	dichloroethane	0.44	0.92	1.4	1.8	ref 24
	TiCl ₄	benzene				2.0	ref 25
$(k_t/k_p)10^2$	CF ₃ SO ₃ H	dichloroethane	0.7-1.4	0.6-1.2	0.7-2.6	0.8-2.5	this work
	H ₂ SO ₄ ^a	dichloroethane	0.38	0.56	0.72	0.88	ref 24

^a Interpolated values from the data at 0, 25, and 30 °C.

made possible the determination of the rate constants of the elementary steps.

Acknowledgment. We are indebted to Professor H. Kobayashi of Kyushu University for fluorine analysis.

References and Notes

- (1) Contribution No. 535 from the Department of Organic Synthesis.
- (2) M. de Sorigo, D. C. Pepper, and M. Szwarc, *Chem. Commun.*, 419 (1973).
- (3) D. C. Pepper, *Makromol. Chem.*, **175**, 1077 (1974).
- (4) J. P. Lorimer and D. C. Pepper, *Proc. R. Soc. London, Ser. A*, **351**, 551 (1976).
- (5) T. Kunitake and K. Takarabe, *J. Polym. Sci., Polym. Symp.*, **56**, 33 (1976).
- (6) T. Kunitake and K. Takarabe, *Polym. J.*, **10**, 105 (1978).
- (7) M. Sawamoto and T. Higashimura, *Macromolecules*, **11**, 328 (1978).
- (8) M. Sawamoto and T. Higashimura, *Macromolecules*, **11**, 501 (1978).
- (9) M. Sawamoto, T. Masuda, and T. Higashimura, *Makromol. Chem.*, **177**, 2995 (1976).
- (10) T. Anfalt and D. Jagner, *Anal. Chim. Acta*, **70**, 365 (1974).
- (11) P. J. Reilly and D. C. Pepper, *Proc. Chem. Soc., London*, 460 (1961).
- (12) C. G. Overberger and M. C. Newton, *J. Am. Chem. Soc.*, **82**, 3622 (1960).
- (13) T. Higashimura and S. Okamura, *Kobunshi Kagaku*, **13**, 397 (1956), and the subsequent papers by these authors.
- (14) P. H. Plesch, *J. Chem. Soc.*, **1953**, 1662.
- (15) D. H. Jenkinson and D. C. Pepper, *Proc. R. Soc. London, Ser. A*, **263**, 82 (1961).
- (16) J. T. Atkins and F. W. Billmeyer, Jr., *J. Phys. Chem.*, **63**, 1966 (1959).
- (17) C. F. Endres, V. G. Kamath, and C. G. Overberger, *J. Am. Chem. Soc.*, **84**, 4813 (1962).
- (18) G. V. Schulz and G. Harborth, *Makromol. Chem.*, **1**, 106 (1947).
- (19) The molecular weight of the quenched polymer was determined by gel permeation chromatography. The calibration curve obtained by using commercial, monodisperse polystyrenes ($M_n = 900, 2030, 4080, 10500$, and 19800) tends to deviate from linearity at the lower end of molecular weight ($M_n \lesssim 2000$), and the molecular weight is underestimated in this region. Since the underestimation is larger at smaller molecular weight (i.e., at higher conversion in the present case), k_t/k_p should be smaller in the Schulz–Harborth plot, and k_{tm}/k_p may be larger by a factor of about 2.
- (20) K. Takarabe, unpublished results.
- (21) C. C. Lee and D. Ungar, *Can. J. Chem.*, **51**, 1497 (1973).
- (22) T. Higashimura and M. Sawamoto, *Polym. Bull.*, **1**, 11 (1978).
- (23) T. Kunitake and K. Takarabe, *Macromolecules*, following paper.
- (24) M. J. Hayes and D. C. Pepper, *Proc. R. Soc. London, Ser. A*, **263**, 63 (1961).
- (25) S. Okamura, T. Higashimura, and I. Sakurada, *Kogyo Kagaku Zasshi*, **61**, 1640 (1958).
- (26) M. Chmelir, *Makromol. Chem.*, **176**, 2099 (1975).
- (27) M. Chmelir, N. Cardona, and G. V. Schulz, *Makromol. Chem.*, **178**, 169 (1977).

Determination of Rate Constants of Free-Ion and Paired-Ion Propagations in the Cationic Polymerization of Styrene by Trifluoromethanesulfonic Acid¹

Toyoki Kunitake* and Kunihide Takarabe

Department of Organic Synthesis, Faculty of Engineering, Kyushu University, Fukuoka 812, Japan. Received August 6, 1979

ABSTRACT: The propagation step of the cationic polymerization of styrene was studied in detail with the $\text{CF}_3\text{SO}_3\text{H}$ initiator in dichloroethane at -1 to 30°C . The apparent rate constant of propagation $k_{p,\text{app}}$ was estimated from the time course of the carbocation (P^+) formation and monomer consumption by the combination of stopped-flow spectroscopy and the rapid quenching technique. Then $k_{p,\text{app}}$ was separated into the rate constants of the free-ion and paired-ion propagations (k_p^+ and k_p^\pm) on the basis of the dependence of $k_{p,\text{app}}$ on $[\text{P}^+]$ and of the effect of a common ion salt. The values of k_p^+ and k_p^\pm were $(2\text{--}30) \times 10^5 \text{ M}^{-1} \text{ s}^{-1}$ and $(0.4\text{--}1.2) \times 10^5 \text{ M}^{-1} \text{ s}^{-1}$, respectively, in the temperature range studied. The ratio k_p^+/k_p^\pm was 6–24, which is much smaller than those observed for the anionic polymerization.

The propagating species in the cationic vinyl polymerization may be composed of the free and paired carbocations. Although the exact nature of the propagating species has been established in the living anionic polymerization of vinyl monomers,² similar analyses were almost impossible in the cationic polymerization, because direct determination of the propagating carbocation could not be done. In recent years, however, direct analyses of the propagating cation were rendered possible in the polymerization of styrenes by stopped-flow/rapid-scan spectroscopy.^{3–10} We described in the preceding paper¹⁰ the determination of the rate constant of the elementary steps (initiation, propagation, chain transfer, and termination) in the cationic polymerization of styrene by trifluoromethanesulfonic acid as studied by stopped-flow/rapid-scan spectroscopy and by the rapid quenching (flow) technique.

As a next step, we conducted a detailed analysis of the propagating process and report the results in this paper. The rate constant of propagation for the free and paired cations could be separated on the basis of the effect of a common ion salt and of the rate dependence on the concentration of the propagating species.

Experimental Section

Materials and the polymerization procedure are described in the accompanying paper in detail.¹⁰ The reaction was followed by a stopped-flow/rapid-scan spectrophotometer (Union Giken Co., Model RA 1300). The stopped-flow and flow (quenching) studies were carried out in the same apparatus by using a special attachment RA 416.

Results and Discussion

Determination of the Apparent Rate Constant of Propagation. It is established in the cationic polymeri-